

reduction of the O₂-evolving center to the S₋₁ state, under similar conditions.

A possible general mechanism for the reaction of hydroxylamine with the O₂-evolving center in dark-adapted PSII membranes, based on the evidence presented in this paper and the results reviewed above, involves at least three steps. The reaction of a hydroxylamine molecule with the O₂-evolving center in the S₁ state would initially produce the S₋₁ species, as described above in eq 3 and 4. Then, a second hydroxylamine molecule would bind at the Cl⁻-binding site and react at a slower rate with the S₋₁ species, reducing the O₂-evolving center to a yet lower oxidation state. According to the model proposed by Brudvig and Crabtree,¹⁴ the Mn complex is most likely a Mn^{IV}₃-Mn^{III} complex in the S₂ state. The S₋₁ state would then be a Mn^{III}₄ complex. Thus, further reduction of the S₋₁ state by hydroxylamine would necessitate production of a Mn^{II} ion in the Mn tetramer. It is well-known that Mn^{II} complexes are relatively labile, owing to a lack of a ligand field stabilization energy.³⁴ We propose, then, that the coordination of hydroxylamine at a sterically hindered Cl⁻-binding site in the O₂-evolving center in the S₁ state precedes the reduction of the Mn complex by hydroxylamine and that the lability of the Mn complex increases as the tetramer is increasingly reduced. This proposal accounts for the inhibition of the Mn-depletion reaction in hydroxylamine-treated thylakoid membranes under moderate intensities of illumination;³⁵ the S₋₁ state intermediate would be oxidized to a less labile oxidation state while under illumination, thus preventing the loss of functional Mn from the O₂-evolving center.

The binding of primary amines to the O₂-evolving center appears to be influenced by the same factors that control the rate of the reaction of hydroxylamines with the Mn complex. First, the Cl⁻ concentration affects the ability of NH₃ and CH₃NH₂ to bind at the type 2 binding site. This result suggests that primary amines displace Cl⁻ from its binding site in a manner like that proposed in eq 3 for the equilibrium involved in the reaction of hydroxylamines with the Mn complex. We have described the competition of amines and Cl⁻ at the type 2 binding site in detail elsewhere;²⁴ the binding of NH₃, CH₃NH₂, and F⁻ in the S₁ state affects the structure of the Mn complex in a manner indistin-

guishable from the effects of depletion of Cl⁻ from the O₂-evolving center. Second, similar steric factors appear to influence the binding of primary amines to the type 2 binding site and the rate constant for the hydroxylamine reaction. Our previous failure to detect the binding of bulky primary amines such as Tris to the O₂-evolving center, even at low Cl⁻ concentrations, is completely consistent with the steric restriction implied by the approximately 17-fold reduction in the rate constant of the hydroxylamine reaction upon *N*-methyl substitution of hydroxylamine. Last, both the primary amines and the hydroxylamines bind to the O₂-evolving center as free-base species, as indicated by the increasing degree of amine inhibition of O₂ evolution¹² and the increasing rate constant for the hydroxylamine reaction with increasing basicity. It is likely, then, that the hydroxylamines and primary amines compete with Cl⁻ for a common site.

The location of this Cl⁻-binding site is likely to be quite near to the Mn complex, since an electron is transferred in a facile manner from a bound hydroxylamine species to the Mn complex. This proximity of the Mn complex to the Cl⁻-binding site could also account for the stabilization by NH₃ and CH₃NH₂ of the form of the Mn complex exhibiting the S₂-state *g* = 4.1 EPR signal; a small, local protein conformational change caused by displacement of Cl⁻ could alter the exchange interactions in the Mn complex,² causing a conversion from the normally observed S₂-state multiline EPR signal to the S₂-state *g* = 4.1 EPR signal. The action of Cl⁻ as a cofactor of photosynthetic O₂ evolution²⁸ could well be due to the maintenance of a preferred protein conformation near the Mn complex. Removal of Cl⁻ from the O₂-evolving center could interfere with the accumulation of oxidizing equivalents, as has been observed in the experiments of Theg et al., Itoh et al., and Ono et al.,³⁶ by perturbing the structure of the Mn complex.²⁴

Acknowledgment. This work was supported by the National Institutes of Health (Grant GM32715). G.W.B. is the recipient of a Camille and Henry Dreyfus Teacher-Scholar Award and an Alfred P. Sloan Fellowship. We thank George Cheniae for several helpful comments concerning this work.

(34) Cotton, F. A.; Wilkinson, G. *Advanced Inorganic Chemistry*; Wiley: New York, 1980; p 739.

(35) Sharp, R. R.; Yocum, C. F. *Biochim. Biophys. Acta* 1981, 635, 90-104.

(36) (a) Itoh, S.; Yerkes, C. T.; Koike, H.; Robinson, H. H.; Crofts, A. R. *Biochim. Biophys. Acta* 1984, 766, 612-622. (b) Theg, S. M.; Jursinic, P. A.; Homann, P. H. *Biochim. Biophys. Acta* 1984, 766, 636-646. (c) Ono, T.; Zimmermann, J.-L.; Inoue, Y.; Rutherford, A. W. *Biochim. Biophys. Acta* 1986, 851, 193-201.

Exciplexes of Ruthenium(II) α -Diimine Complexes with Silver(I)

N. P. Ayala,[†] J. N. Demas,^{*†} and B. A. DeGraff^{*†}

Contribution from the Departments of Chemistry, University of Virginia, Charlottesville, Virginia 22901, and James Madison University, Harrisonburg, Virginia 22807.

Received August 5, 1987

Abstract: Luminescence "quenching" of RuL₃²⁺ (L = 2,2'-bipyridine and 4,7-dimethyl-1,10-phenanthroline) photosensitizers by Ag⁺ in aqueous solutions is shown to proceed, not by oxidative electron transfer quenching as previously believed, but predominantly by formation of luminescent exciplexes. Photochemical formation of Ag⁰(aq) is <0.02 in water and <0.05 in acetonitrile. Both a normal bimolecular exciplex, *(RuL₃|Ag)³⁺, and a rare termolecular *(RuL₃|Ag₂)⁴⁺ exciplex are observed. This appears to be the first example of an exciplex formed by a Ru(II) α -diimine sensitizer and of a termolecular metal complex exciplex. Spectral properties of the exciplexes, energetics, and dynamics for these systems are discussed.

Platinum metal complex photosensitizers are invaluable mechanistic tools and promise to function as the photon antenna in photochemical energy conversion or other photocatalytic systems. Much of the work has been devoted to the original Ru-

(bpy)₃²⁺ (bpy = 2,2'-bipyridine) complex and its analogues. These sensitizers offer considerable flexibility due to the ease of altering their properties by modifying the α -diimine ligand in order to tune excited state energies or redox potentials.¹ A second approach

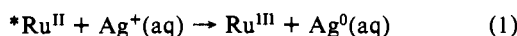
[†]University of Virginia.

[‡]James Madison University.

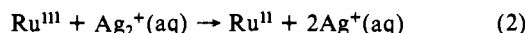
(1) Kalyanasundaram, K. *Chem. Soc. Rev.* 1978, 7, 432.

to controlling properties, particularly the radiative and radiationless rate constants, is by altering the local environment.² A major thrust of our efforts has involved studies of the effect of solvent and microenvironment on the photochemistry and photophysics of metal complexes.³

As part of our study on the effect of solvents on electron transfer reactions, we examined the Ag⁺ quenching of Ru(II) photosensitizers. The Ru(bpy)₃²⁺-Ag⁺ system has been studied by Whitten and co-workers.⁴⁻⁷ They attributed the apparent quenching to oxidative electron transfer.



In the absence of scavengers, a transient attributed to Ru(III) was observed with flash photolysis, but no permanent chemistry was seen. The absence of permanent photochemistry was attributed to the fast back reaction



where Ag₂⁺ originates from the well-known rapid reaction of Ag⁰ with excess Ag⁺.⁸

In water and in acetonitrile, Whitten et al.⁴⁻⁷ found that quenching rate constants were relatively low and positive deviations from Stern-Volmer kinetics were observed at high Ag⁺ concentrations. In the presence of scavengers, Ag metal was formed with yields of ~0.04.⁵

In order to examine the detailed mechanism of silver ion quenching, we conducted a solvent dependency study on mixtures of water and acetonitrile with various α-diimine ruthenium(II) complexes. It became clear that many of our observations were experimentally and interpretationally inconsistent with the earlier reports. After careful analysis of emission spectra, lifetimes, flash photolysis results, and oxygen quenching, we concluded that Ag⁺ does not significantly quench the excited state by oxidative electron transfer. The apparent luminescence "quenching" arises from formation of both bimolecular and termolecular exciplexes with Ag⁺. This is the first example of a Ru(II) photosensitizer based exciplex and of a termolecular metal complex exciplex.

Experimental Section

Materials. AgNO₃, 4,7-dimethylphenanthroline (4,7-Me₂phen), and Ru(bpy)₃Cl₂·6H₂O were purchased from G. F. S. Chemical Co. RuCl₃·6H₂O and LiNO₃ from Alpha were used as received. Ru(bpy)₃(ClO₄)₂ was prepared from Ru(bpy)₃Cl₂ by metathesis. Ru(4,7-Me₂phen)₃(ClO₄)₂ was prepared as described previously.⁹ Triethylamine from Aldrich Chemical Co. was redistilled immediately prior to use. Polyvinyl alcohol (PVA) was also from Aldrich Chemical Co. Deionized water was distilled from KMnO₄/KOH.

Luminescence and Absorption Measurements. Excited state lifetimes (τ) were determined with the decay time instrument described earlier.^{9,10} The emission decays were first order as shown by linear least-squares plots of log I versus time over at least two mean lifetimes. There was no emission wavelength dependence (600 and 640 nm) to the lifetime. Precision in the lifetime determinations was better than ±20 ns.

Room temperature absorption spectra were recorded on a Cary 17 spectrometer and were blank corrected. Spectra were measured for

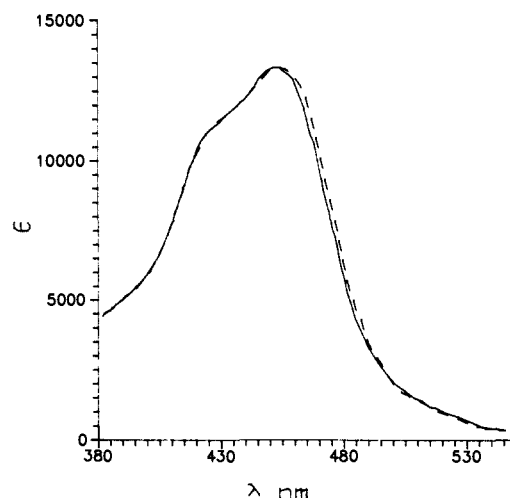


Figure 1. Absorption spectra of Ru(bpy)₃²⁺ in aqueous 3.0 M LiNO₃ (—) and 1.5 M AgNO₃/1.5 M LiNO₃ (---).

solutions containing equimolar amounts of the Ru(II) complexes in pure water, in 3.0 M LiNO₃, and in 1.5 LiNO₃/1.5 M AgNO₃. The complexes had very limited solubility at high nitrate concentrations, and spectra were measured in 10-cm cells.

Emission and excitation spectra were recorded on an SLM 8000 single-photon counting spectrofluorimeter equipped with a cooled R928 PMT and PC interface and controlling computer. Emission spectra were recorded with an excitation wavelength of 457 nm with an excitation bandpass of 16 nm and an emission bandpass of 4 nm. Excitation spectra were uncorrected. Unless otherwise indicated, all samples were deaerated with solvent saturated nitrogen. All spectra were background subtracted with suitable blanks. Emission spectra were corrected for the spectral sensitivity of the instrument. All measurements were made at 25.0 ± 0.5 or 6 ± 1 °C.

Emission spectra over the range 500–800 nm were recorded at different [AgNO₃] (0–1.5 M); the total [NO₃⁻] concentration was fixed at 3.0 M with LiNO₃. Lifetime titrations were carried out under the same conditions.

Quenching Measurements. As we found that the emission spectra of the complexes varied as a function of [Ag⁺], a normal Stern-Volmer plot of intensity at a single wavelength was inappropriate. We, therefore, determined the relative quantum yield by measuring the area under the entire corrected emission spectrum, A. This was used in place of the normal intensity at a single emission wavelength.

The emission spectra of Ru(II) complexes in the presence or absence of Ag⁺ extends beyond the 800-nm range of our instrument. To determine the contribution to the total emission arising from this long wavelength portion, we graphically extrapolated the emission and added the additional portion to the total area. The correction was less than 4% of the unquenched area.

Oxygen quenching measurements were performed by measuring the integrated emission intensities of deaerated and aerated samples at different [Ag⁺]. Apparent Stern-Volmer, K_{SV}^{app} , and bimolecular, oxygen quenching constants, k_2^{app} , were determined from

$$K_{SV}^{app} = [(A_0/A) - 1]/[O_2] \quad (3)$$

$$k_2^{app} = K_{SV}^{app}/\tau_{obsd}([O_2] = 0) \quad (4)$$

where A_0 is the corrected area under the unquenched emission, [O₂] was the oxygen concentration in the media (assumed to be the same as for pure water), and $\tau_{obsd}([O_2] = 0)$ is the lifetime in the absence of oxygen.

Flash Photolysis. Flash photolysis measurements were performed with an instrument described earlier.¹¹ An 18-cm path, double-walled cell was used. Excitation was limited to 400–460 nm by a sodium nitrite-Cu(NH₃)₄²⁺ solution filter in the outer jacket. Absorption changes were monitored at 436 nm, which is near the absorption maximum of the Ru(II) sensitizer and in a region of weak absorption of the anticipated Ru(III) product ($\Delta\epsilon \approx 10\,600\text{ M}^{-1}\text{ cm}^{-1}$). For quantum yield determinations flash actinometers with either the ferric^{11a} ion or paraquat^{11b-d} quenched Ru(bpy)₃²⁺ systems were used.

(11) (a) Hauenstein, B., Jr.; Dressick, W.; Demas, J. N.; DeGraff, B. A. *J. Phys. Chem.* **1984**, *88*, 2418. (b) Bock, C. R.; Meyer, T. J.; Whitten, D. J. *J. Am. Chem. Soc.* **1974**, *96*, 4710. (c) Kalyanasundaram, K. *Coord. Chem. Rev.* **1982**, *46*, 159. (d) Gaines, G. L., Jr. *J. Phys. Chem.* **1979**, *83*, 3088.

(2) (a) Kalyanasundaram, K. *Photochemistry in Microheterogeneous Systems*; Academic: New York, 1987. (b) Kober, E. M.; Meyer, T. J. *Inorg. Chem.* **1985**, *24*, 106.

(3) (a) Dressick, W. J.; Cline, J. B.; Demas, J. N.; DeGraff, B. A. *J. Am. Chem. Soc.* **1986**, *108*, 7567. (b) Reitz, G. A.; Dressick, W. J.; Demas, J. N.; DeGraff, B. A. *Ibid.* **1986**, *108*, 5344. (c) Snyder, S. W.; Raines, D. E.; Rieger, P. T.; Demas, J. N.; DeGraff, B. A. *Langmuir* **1985**, *1*, 548.

(4) Foreman, T. K.; Giannotti, C.; Whitten, D. G. *J. Am. Chem. Soc.* **1980**, *102*, 1171.

(5) Chandrasekaran, K.; Foreman, T. K.; Whitten, D. G. *Nouv. J. Chim.* **1981**, *5*, 275.

(6) Foreman, T. K. Ph.D. Dissertation, University of North Carolina at Chapel Hill, 1981.

(7) Foreman, T. K.; Boniha, J. B. S.; Whitten, D. G. *J. Phys. Chem.* **1982**, *86*, 3436.

(8) (a) Pukies, J.; Roekke, W.; Heinglein, A. *Ber. Bunsenges. Phys. Chem.* **1968**, *72*, 842. (b) Heinglein, A. *Angew. Chem.* **1979**, *91*, 449. (c) Heinglein, A. *Angew. Chem.* **1979**, *91*, 449.

(9) (a) Hauenstein, B. L., Jr.; Mandal, K.; Demas, J. N.; DeGraff, B. A. *Inorg. Chem.* **1984**, *23*, 1101. (b) Dressick, W. J.; Raney, K. W.; Demas, J. N.; DeGraff, B. A. *Ibid.* **1984**, *23*, 875.

(10) (a) Turley, T. J. M.S. Thesis, University of Virginia, 1980. (b) Turley, T. J.; Demas, J. N.; Demas, D. J. *Anal. Chim. Acta*, in press.

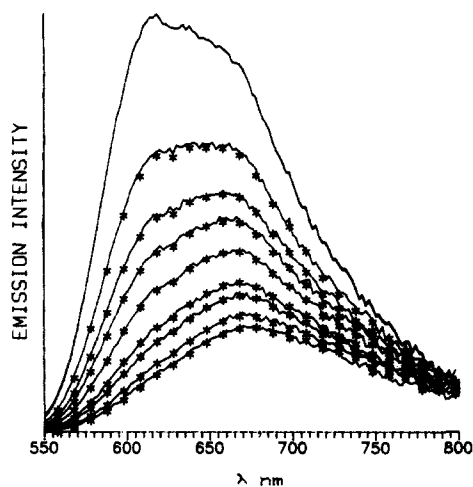


Figure 2. Emission spectra of $\text{Ru}(\text{bpy})_3^{2+}$ versus $[\text{Ag}^+]$. The ionic strength is held at 3.0 M with LiNO_3 . The asterisks are the calculated best fit with the three-component model (see text); every fifth point is shown. The intensities of the curves decrease in peak emission intensity as $[\text{Ag}^+]$ increases. The silver concentrations are 0.0, 0.09, 0.176, 0.25, 0.375, 0.6, 0.75, 1.125, and 1.50 M.

Measurements were made on solutions of $\text{Ru}(\text{bpy})_3^{2+}$ and 0.25, 0.5, and 1.5 M AgNO_3 in pure water or with 0.01 M nitric acid. Measurements were made at both fixed 3 M ionic strength and also without extra electrolyte. Additional similar experiments were done in water with $\text{Ru}(4,7\text{-Me}_2\text{phen})_3^{2+}$ as the sensitizer. Measurements were also made in the presence of 1% aqueous PVA (MW = 14 000 Da). With use of acetonitrile with $\text{Ru}(\text{bpy})_3^{2+}$ as the sensitizer, experiments were conducted at 1.0 and 4.0 M AgNO_3 . Deoxygenation was either by an inert gas purge or 5 cycles of freeze-pump-thaw.

Steady-State Photolysis. Continuous photolysis experiments were done with a 100-W Hg/Xe arc where the output was filtered through 10 cm of water and either Pyrex glass or a No. 3060 cutoff filter in conjunction with 10 cm of 1 M NaNO_2 . All photolysis vessels were of Pyrex glass. Samples were deaerated by either nitrogen purging for 30 min or, in the case of PVA solutions, 5 freeze-pump-thaw cycles. Photolysis aliquots were 15 mL. All experiments were done at room temperature, 22–24 °C. Solutions were prepared immediately prior to use. Both AgNO_3 and AgClO_4 were used as sources of Ag^+ .

Fitting Procedures. A number of different nonlinear models were used to fit the results. Fits were performed with a Pascal version of a simplex routine described earlier.¹² Computations were done on an AT&T computer equipped with an 8087 math coprocessor.

Results

Figure 1 shows the absorption spectra of $\text{Ru}(\text{bpy})_3^{2+}$ in 3.0 M LiNO_3 and in 1.5 M LiNO_3 –1.5 M AgNO_3 . The 3 M NO_3^- media exhibit a small 3–5 nm red shift compared to the pure water spectrum. The observed absorption spectra in the two nitrate media are indistinguishable. Similar results were obtained for $\text{Ru}(\text{Me}_2\text{phen})_3^{2+}$. Figure 2 shows the emission spectra of $\text{Ru}(\text{bpy})_3^{2+}$ as a function of $[\text{Ag}^+]$ at 3 M ionic strength. A dramatic 60 nm red shift and decrease in the peak emission intensity is observed as the $[\text{Ag}^+]$ increases. Similar spectral changes are observed if the experiment is done by adding only AgNO_3 to a solution of the complex in pure water, but the decrease in emission intensity is even greater. Again, similar results were obtained for $\text{Ru}(\text{Me}_2\text{phen})_3^{2+}$.

The emission spectra in 3 M LiNO_3 may be slightly red shifted relative to that in pure water. This is consistent with the absorption shifts.

Excitation spectra for $\text{Ru}(\text{bpy})_3^{2+}$ in pure water, in 3 M LiNO_3 , and in 1.5 M LiNO_3 –1.5 M AgNO_3 yield results analogous to the absorption spectra. The two nitrate systems are virtually indistinguishable from each other.

Figure 3 shows Stern–Volmer plots for the integrated emission intensity and the luminescence lifetimes as a function of $[\text{Ag}^+]$

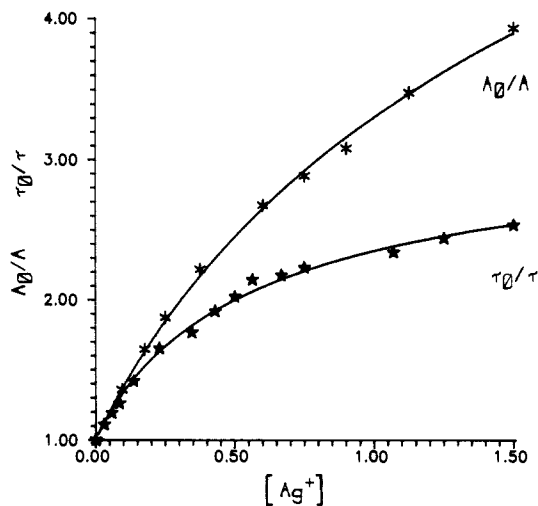


Figure 3. Intensity (*) and lifetime (★) Stern–Volmer quenching plots for the $\text{Ru}(\text{bpy})_3^{2+}$ – Ag^+ system at 3 M ionic strength. A is the total area under the corrected emission spectrum. The solid curves are the calculated best fits based on the three-component model.

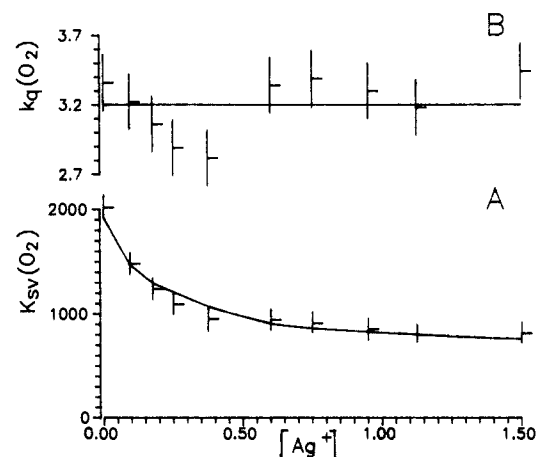


Figure 4. Apparent Stern–Volmer (A) and bimolecular oxygen quenching constants (B) for $\text{Ru}(\text{bpy})_3^{2+}$ as a function of $[\text{Ag}^+]$ at 3 M ionic strength. The solid curve in A is the calculated fit with the three-component model and assuming a species invariant bimolecular quenching constant.

for $\text{Ru}(\text{bpy})_3^{2+}$ at 3 M ionic strength. The relative changes in the lifetime, τ_0/τ , are less than the changes in the relative quantum yields, A_0/A . Both curves exhibit strong negative deviations from linear Stern–Volmer behavior. Similar results were obtained for $\text{Ru}(\text{Me}_2\text{phen})_3^{2+}$.

Figure 4 shows oxygen quenching results for $\text{Ru}(\text{bpy})_3^{2+}$ at 3 M ionic strength. The apparent oxygen Stern–Volmer quenching constants and bimolecular quenching constants are shown versus $[\text{Ag}^+]$. The large change in K_{SV} is largely due to the shortening of τ . The oxygen bimolecular quenching constant is not strongly dependent on $[\text{Ag}^+]$ and, given our large errors, may be constant. Again similar results were obtained for $\text{Ru}(\text{Me}_2\text{phen})_3^{2+}$.

Despite the use of forcing conditions in the flash photolysis experiments, we never detected any transients that could be ascribed to production of Ru(III) via electron transfer quenching by Ag^+ in either solvent. Using as a basis of comparison systems with known electron transfer efficiencies,¹¹ we can conservatively estimate that any production of Ru(III) by Ag^+ has a yield of <0.02 in water and <0.05 in acetonitrile. While at high pulse energies (580 J) there was a small amount of transient bleaching, experiments without added Ag^+ showed this to be completely due to the well-known, slow reversible process.¹³ Our flash results

(12) (a) Daniels, R. W. *An Introduction to Numerical Methods and Optimization Techniques*; North Holland, Inc.: New York, 1978. (b) Demas, J. N. *Excited State Lifetime Measurements*; Academic: New York, 1983.

(13) (a) Durham, B.; Caspar, J. V.; Nagle, J. K.; Meyer, T. J. *J. Am. Chem. Soc.* **1982**, *104*, 4803. (b) Meisel, D.; Matheson, M. S.; Mulac, W. A.; Rabani, J. *J. Phys. Chem.* **1977**, *81*, 1449.

appear to be inconsistent with those of Foreman and Whitten,⁴ and we cannot account for these discrepancies despite efforts by both groups to resolve the question. Our 0.02 limit for Ag⁰ formation is, however, similar to the low Ag metal formation efficiencies (0.04) reported in scavenging experiments.⁵ It is also possible that Ag⁰ formation by scavengers arises from direct reaction of the exciplex with the scavenger.

In the steady state irradiation experiments without triethylamine, we found no evidence for photochemical production of Ag metal during a 30-min irradiation at any excitation wavelength (300–500 nm with 1.0 M AgNO₃ or AgClO₄) using either deaerated water or acetonitrile. This was true with or without Ru(bpy)₃²⁺. With added photosensitizer and 0.01 M triethylamine with a carefully restricted excitation window ($\lambda > 400$ nm), there was slow production of Ag metal in the presence or absence of light. The extent of the photochemically sensitized contribution was not ascertained, but the yields are low.

Significantly more efficient production of Ag metal in acetonitrile occurred if we expanded our photolysis window (Pyrex filters, $\lambda > 300$ nm) and added 0.01 M triethylamine. This was true whether or not Ru(bpy)₃²⁺ was present. With these experimental conditions, nitrate, Ag⁺, and triethylamine absorb light. A slow thermal production of colloidal silver was also observed in the dark. On irradiation, however, production of colloidal silver was greatly accelerated as indicated by Tyndall scattering and formation of a silver mirror. Attempts to conduct a similar experiment with aqueous solutions were thwarted by immediate precipitation of the silver on addition of triethylamine.

We also examined the effect of using PVA to sequester the Ag atoms in aqueous solution.⁵ A solution of 1.0 M AgNO₃ in 1% aqueous PVA was degassed and irradiated as above (>300 nm). After 30 min the solution showed distinct Tyndall scattering and a yellow color. This same effect could be produced thermally in the dark, though much more slowly. These observations were made without benefit of sensitizer. Our steady illumination results are qualitatively in accord with those reported earlier.^{4–6} Photochemically assisted production of Ag⁰ in the presence of sensitizer and suitable scavenger in acetonitrile appears to occur with very low efficiency. However, the system is complex and it is clear that if great care is not taken in restricting the photolysis window and accounting for thermal processes, the interpretation is clouded.

The red shift in the absorption spectra in nitrate-containing media is indicative of ion pairing between the Ru(II) complex and the NO₃⁻.¹⁴ From the absence of spectral changes on replacing LiNO₃ with AgNO₃, we conclude that there is no ground state association of RuL₃²⁺ with Ag⁺. We further conclude that the primary species seen in absorption and excited in emission is the nitrate ion-paired complex.

The substantial emission spectral changes that occur on addition of Ag⁺ leave no doubt that there is at least one new emissive species present. In the absence of any evidence for ground-state association with Ag⁺, we conclude that the new emissive species are exciplexes of the photosensitizer with Ag⁺.

We cannot absolutely rule out the possibility that there is a ground-state Ag⁺ association complex with the sensitizer, but we consider it unlikely. The emission shifts by at least 60 nm on addition of Ag⁺, yet there is no detectable shift in the absorption spectrum. The metal-to-ligand charge-transfer (MLCT) band is very susceptible to environmental factors as seen by the readily observed subtle effect of formation of a NO₃⁻ ion pair. Because of the large spectral consequences of excited state interactions, ground-state complexation, if present, should be mirrored by analogous changes in the 450-nm MLCT absorption band. The absence of such changes leads us to conclude that there is no ground-state complexation.

While not definitive, the excitation spectra are consistent with either of two things. The excitation spectra are invariant on monitoring at 600 or 640 nm; these wavelengths are near the silver free and high silver emission maxima. This shows that if there is ground-state complexation, photoselection of different forms

in the ground state is washed out by rapid equilibration in the excited state. Alternatively, if there is no ground-state complex, the excitation spectra provide no further information.

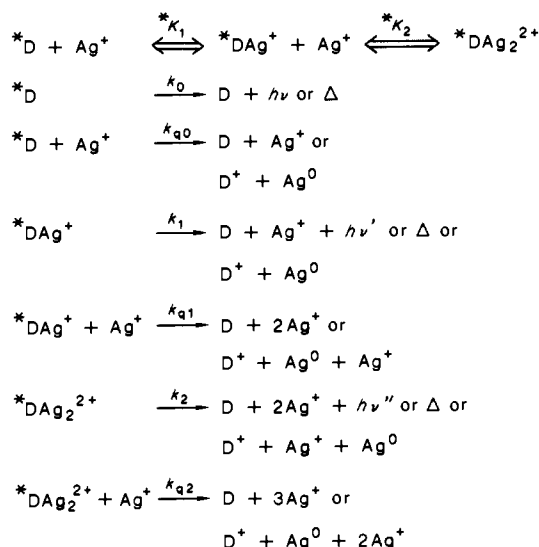
Discussion

Any successful model must account qualitatively and quantitatively for the spectral shifts, the changes in emission intensities and lifetimes, and the oxygen effects. We considered and rejected a number of simple models because of their failure to fit one or more of these features.

We immediately rejected any model that involved only bimolecular or static quenching of our sensitizers. Static quenching should yield positive deviations in the intensity curves and linear lifetime plots; these predictions are inconsistent with our data (Figure 3). The large emission shifts prove that there is at least one new excited state species.

Below is our Scheme I and an explanation as to why we rejected subsets of this scheme. This model includes both monomolecular decay paths and direct bimolecular quenching paths to the ground state.

Scheme I



where *D represents the excited sensitizer, k_i 's are the rate constants for decay of each excited state species, and k_{qi} 's are bimolecular quenching constants for deactivation of the excited state species by Ag⁺. We show formation of a mono *DAg⁺ exciplex and a termolecular exciplex, *DAg₂²⁺, and associated excited state equilibrium constants for their formation. We justify inclusion of this termolecular species later.

In all subsequent analyses we assume that an equilibrium exists between the excited species. This is reasonable given the very long excited state lifetimes (>150 ns) and the high silver concentrations, which ensure many excited state collisions before decay. Further, the decay curves show no deviations from single exponentiality that might be expected if equilibration were incomplete. Finally, as we will show, an equilibrium model fits all of our data.

The proposed model of Scheme I yields the following equations for the observed lifetime and emission spectra:

$$I(\lambda) = Z \sum f_i I_i(\lambda) \quad (5a)$$

$$1/\tau_{\text{obsd}} = \sum f_i (1/\tau_i) \quad (5b)$$

$$k_i = (1/\tau_i) \quad (5c)$$

$$f_0 = 1/(1 + *K_1[Ag^+] + *K_1*K_2[Ag^+]^2) \quad (5d)$$

$$f_1 = *K_1[Ag^+]/(1 + *K_1[Ag^+] + *K_1*K_2[Ag^+]^2) \quad (5e)$$

$$f_2 = *K_1*K_2[Ag^+]^2/(1 + *K_1[Ag^+] + *K_1*K_2[Ag^+]^2) \quad (5f)$$

$$1/\tau_i = k_i + k_{qi}[Ag^+] \quad (5g)$$

$$Z = [\sum f_i/\tau_i]/\{\sum [1 + k_{qi}\tau_i[Ag^+]](f_i/\tau_i)\} \quad (5h)$$

where the summations are over the number of components. The

(14) Vining, J.; Caspar, J. V.; Meyer, T. J. *J. Phys. Chem.* **1985**, *89*, 1055.

i 's denote the number of Ag^+ 's bound to the sensitizers, $I(\lambda)$ and τ_{obsd} are the observed emission spectrum and lifetime, respectively, f 's are the fraction of each component existing in the excited state manifold, τ 's are the lifetimes of each component if there were no coupling between excited state species, and k_q 's are the bimolecular Ag^+ quenching rate constants for each component. The $I_i(\lambda)$'s are the spectra that would be observed if only the i th component were present and there were no bimolecular quenching to back the ground state by Ag^+ or interconversion to the other forms. Z is the degree of Ag^+ quenching of the entire excited state manifold via deactivation of the different excited state species.

We now discard untenable models. In our first fitting attempts we assumed a minimal system that involved only *D and $^*D\text{Ag}^+$ ($^*K_2 = 0$). This is the simplest scheme that can yield spectral shifts. There are two variations of the model. We could have no Ag^+ quenching of the excited states or Ag^+ could directly deactivate one or more of the excited species.

First we assumed that there is no bimolecular quenching (k_q 's = 0). This model totally failed to fit the I versus $[\text{Ag}^+]$ curves at different wavelengths or the τ versus $[\text{Ag}^+]$ and was discarded.

Next we introduced bimolecular quenching of *D and $^*D\text{Ag}^+$ by Ag^+ ($k_{q1} \neq 0$ and $k_{q2} \neq 0$). This model would fit our lifetime data, but not the intensity data. We describe the fitting procedure and the reason for rejection of this model below.

First, we fit the lifetime to eq 5 using two quenching constants. The nonlinear least squares forced k_{q2} to zero. The fit to the lifetime data was excellent with $k_{q2} = 0$, $\tau_1 = 199$ ns, $k_{q1} = 1.26 \times 10^5 \text{ M}^{-1}\text{s}^{-1}$, and $^*K_1 = 1.93 \text{ M}^{-1}$.

This set of parameters failed severely when applied to the emission spectra. However, multiparameter least-squares fitting of real experimental data does not always yield the best parameter estimates that can be applied to other related data sets (i.e., the I versus $[\text{Ag}^+]$ data). To avoid being misled by such artifacts, we examined a range of parameters around the best fit values. There was a range of parameter combinations (except k_{q2} which always went to 0) that gave visually acceptable fits to the lifetime data. We then attempted to use this range of values to fit the intensity curves versus $[\text{Ag}^+]$. While satisfactory fits could be obtained for some combinations of parameters at some wavelengths, no set of parameters yielded fits that were free of severe systematic errors at most or all wavelengths. Thus, a single exciplex system with bimolecular quenching is untenable and must be discarded.

The failure of two-component models to fit the data led to our adoption of the three-component system involving *D , $^*D\text{Ag}^+$, and $^*D\text{Ag}_2^{2+}$. Three components with no direct bimolecular quenching by Ag^+ was the minimum model that fit all of our data. The fitting procedure was involved and we describe it in detail.

In the three-component model, it was necessary to fit *K_1 , *K_2 , τ_1 , τ_2 , and the emission spectra of the two exciplexes ($I_1(\lambda)$ and $I_2(\lambda)$). The spectrum ($I_0(\lambda)$) and decay time (τ_0) for *D were taken as the directly measured values in the absence of Ag^+ .

The procedure used for determining *K_1 and *K_2 depends upon the assumption that $I_2(\lambda)$ can be neglected in a limited spectral region. We chose 540–600 nm. This assumption appears to be a good one since the spectrum of $^*D\text{Ag}_2^{2+}$ is much less intense than the spectrum of $^*D\text{Ag}^+$, $I_1(\lambda)$, in this wavelength region.

Using *K_1 , *K_2 , and $I_1(\lambda)$ as fitting parameters, we performed simplex fits to the I versus $[\text{Ag}^+]$ data using eq 5. Thirty sets of constants were obtained by fitting the data between 540 and 600 nm; the *K_1 's and *K_2 's were averaged. There was no systematic variation in the *K 's with wavelengths. This validates our assumption about the unimportance of $I_2(\lambda)$ in this region.

Having now obtained reliable estimates of the equilibrium constants, we fit all the $I(\lambda)$ data at each wavelength (540 to 800 nm) using $I_1(\lambda)$ and $I_2(\lambda)$ as the fitting parameters while the *K 's were held fixed. In all cases satisfactory fits were obtained; the residuals were randomly distributed with respect to sign and magnitude. The best fit $I_1(\lambda)$ and $I_2(\lambda)$ along with $I_0(\lambda)$ are shown in Figure 5.

The relative areas under the three-emission curves permit us to calculate the absolute luminescence quantum yields for the

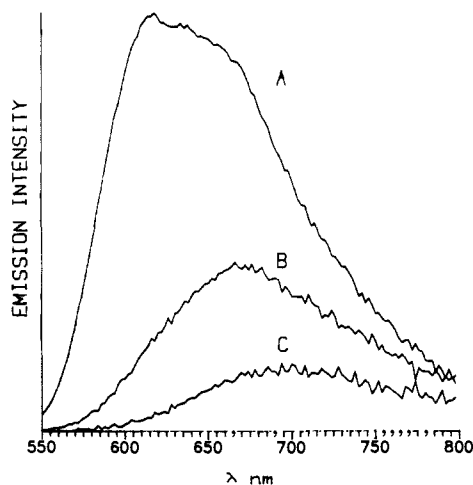


Figure 5. $I_0(\lambda)$ (A) and calculated $I_1(\lambda)$ (B) and $I_2(\lambda)$ (C).

Table I. Quantum Yields, Lifetimes, and Rate Constants for $^*\text{RuL}_3^{2+}(\text{Ag}^+)_x$ Exciplexes

| x | Q | τ (μs) | $k_{\text{nr}} \times 10^{-6}$ (s^{-1}) | $k_t \times 10^{-4}$ (s^{-1}) |
|---|-------------------|--------------------------|---|---|
| $^*\text{Ru}(\text{bpy})_3^{2+}(\text{Ag}^+)_x$ | | | | |
| 0 | 0.048 ± 0.001 | 0.600 | 1.6 ± 0.1 | 8.0 ± 0.2 |
| 1 | 0.019 ± 0.001 | 0.38 | 2.6 ± 0.1 | 5.0 ± 0.1 |
| 2 | 0.007 ± 0.001 | 0.18 | 5.5 ± 0.1 | 3.9 ± 0.1 |
| $^*\text{Ru}(\text{Me}_2\text{phen})_3^{2+}(\text{Ag}^+)_x$ | | | | |
| 0 | 0.082 ± 0.001 | 1.62 | 0.57 ± 0.01 | 5.1 ± 0.2 |
| 1 | 0.023 ± 0.001 | 0.98 | 1.0 ± 0.1 | 2.3 ± 0.1 |
| 2 | 0.010 ± 0.001 | 0.25 | 3.9 ± 0.1 | 4.0 ± 0.1 |

exciplexes. $\text{Ru}(\text{bpy})_3^{2+}$ and $\text{Ru}(\text{Me}_2\text{phen})_3^{2+}$ have luminescence quantum yields of 0.042¹⁵ and 0.0665^{3a} in deaerated pure water. The yields are slightly higher in 3 M LiNO_3 . Using these yields as references and correcting the extrapolation for the portions of the emission extending beyond the range of our instrument, we calculated the yields for the exciplexes (Table I).

As a check on the validity of the two-exciplex model, we recalculated all the emission spectra using the derived $I_1(\lambda)$, $I_2(\lambda)$, *K_1 , and *K_2 . These fits are shown in Figure 2. To avoid cluttering the figure, only every fifth point is displayed, but the remaining points fit equally well. The agreement between all the observed and calculated spectra is excellent, shows no systematic deviations, and is well within our experimental error. We conclude that the two-exciplex model without any direct quenching of the excited states by Ag^+ fully describes our emission results.

We cannot exclude the possibility of the more complex case involving some direct bimolecular quenching of the excited states. However, since these added complexities are not required to fit our data, we limit ourselves to the simpler case. As further support of the absence of direct bimolecular quenching, we find no evidence for a significant photochemical deactivation pathway involving electron transfer.

One reason why earlier workers may have missed the presence of exciplex formation is that the luminescence yields of the exciplexes are lower than that of the parent, and their emissions are red shifted. If one were examining uncorrected emission spectra on an instrument with poor red sensitivity, the large spectral shifts would be lost in the falling red sensitivity of the detector and simple quenching would appear to be present.

Lifetime and Oxygen Quenching Data. If the two-exciplex model is correct, it must also fit our lifetime versus $[\text{Ag}^+]$ and the oxygen quenching data. Further, this fitting has to use a *K_1 and a *K_2 that are consistent with that derived from the intensity data.

To carry out the two-exciplex lifetime fits, we fit $1/\tau_{\text{obsd}}$ versus $[\text{Ag}^+]$ with eq 5; τ_1 and τ_2 were varied and *K_1 and *K_2 were set

Table II. Equilibrium Constants and Thermodynamic Parameters for Formation of Ag(I) Exciplexes with Ruthenium(II) Sensitizers

| RuL ₃ ²⁺ L = | 298 K | | 279 K | | 298 K | | 278 K | |
|---------------------------------------|-----------------------------------|-----------------------------------|-----------------------------------|-----------------------------------|----------------------------|----------------------|----------------------------|----------------------|
| | *K ₁ , M ⁻¹ | *K ₂ , M ⁻¹ | *K ₁ , M ⁻¹ | *K ₂ , M ⁻¹ | ΔH ₁ , kcal/mol | ΔS ₁ , eu | ΔH ₂ , kcal/mol | ΔS ₂ , eu |
| bpy | 6.9 ± 0.5 | 1.1 ± 0.5 | 13 ± 1 | 4 ± 1 | -6 ± 2 | -24 ± 10 | -12 ± 3 | -39 ± 10 |
| Me ₂ phen | 12 ± 1 | 1 ± 0.7 | | | | | | |

to the previously determined values. The best fit τ_1 and τ_2 are tabulated in Table I. The fit to the data is shown in Figure 3. Also, shown in Figure 3 is a best fit to the A_0/A data. The quantum yields derived from this fit agree well with those determined from the more laborious fitting of Figure 2.

In the oxygen-quenching results, the rough invariance of k_2^{app} suggests that even though there are multiple species present versus $[\text{Ag}^+]$, they must all have similar bimolecular quenching constants. We calculated the Stern-Volmer quenching curve based on a species invariant k_2 of $3.3 \pm 0.2 \times 10^9 \text{ M}^{-1} \text{ s}^{-1}$ (the average of all the k_2^{app} 's). The apparent bimolecular Stern-Volmer oxygen-quenching constant is given by

$$K_{\text{SV}}^{\text{app}} = k_2^{\text{app}} \tau_{\text{obsd}}([\text{O}_2] = 0) = k_2 \tau_{\text{obsd}} \quad (6)$$

where τ_{obsd} is given by eq 5b. In Figure 4 the solid line through the experimental $K_{\text{SV}}^{\text{app}}$'s is determined from eq 6 by using the $*K_1$ and $*K_2$ derived earlier. There do appear to be some small systematic deviations between the observed and calculated curves, which are just outside experimental error. This suggests that k_2 may vary somewhat between exciplexes.

The relative constancy of the bimolecular oxygen-quenching constants can be attributed to the large exothermicity ($>1 \text{ eV}$) for energy transfer from all three species to oxygen. This yields a near diffusion controlled rate constant.

Radiative and Nonradiative Rate Constants. The radiative (k_{ri}) and nonradiative (k_{nr}) rate constants for decay of each luminescent species were calculated from the absolute luminescence quantum yields, Q_i 's, and limiting lifetimes, τ_i 's.

$$k_{\text{nr}} = (1 - Q_i) / \tau_i \quad (7a)$$

$$k_{\text{ri}} = Q_i / \tau_i \quad (7b)$$

The rate constants are summarized in Table I.

The nonradiative rate constant increases as more Ag^+ binds to $*\text{D}$. The red shift in the emission spectra with increasing number of bound Ag^+ 's indicates a lower excited state energy in the exciplexes. An increased k_{nr} is then predicted by the energy gap law.^{14,16,17} The k_{nr} 's for the two exciplexes fall on the same energy gap law plot as the data for a large number of other Os(II) and Ru(II) photosensitizers.^{14,17}

There is also a suggestion that k_{r} decreases with the number of bound silvers. For $\text{Ru}(\text{Me}_2\text{phen})_3^{2+}$, Q_2 has very large uncertainties, and no conclusions about k_{r} can be made. A decreased k_{r} would, however, be consistent with the lowering of the state energy and the spin-orbit coupling model proposed earlier.¹⁸

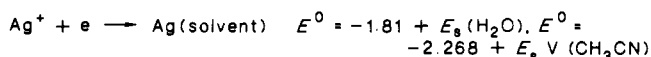
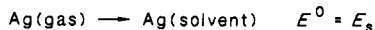
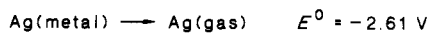
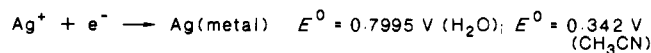
The shapes of the emissions of $*\text{D}$, $*\text{D}\text{Ag}$, and $*\text{D}\text{Ag}^{2+}$ are strikingly similar. Since the $*\text{D}$ emission is a metal-to-ligand charge-transfer emission, we conclude that the $*\text{D}\text{Ag}^+$ and $*\text{D}\text{Ag}_2^{2+}$ likewise exhibit MLCT emissions. This is supported by the similar radiative rate constants for the three Ru(II) species. A ligand localized emission is ruled out by the very low emission energies.

Photochemistry. Our failure to observe transient formation of Ru(III), coupled with our observations regarding the steady irradiation chemistry, suggests that electron-transfer quenching by

Ag^+ is very minimal. The major reason for decreased luminescence of the sensitizers is the formation of exciplexes with lower quantum yields.

We had hoped to estimate the barrier for the electron-transfer reaction so that a prediction of electron-transfer rates could be made. With quenching rates of $3.5 \times 10^6 \text{ M}^{-1} \text{ s}^{-1}$ in water and $1.1 \times 10^5 \text{ M}^{-1} \text{ s}^{-1}$ in acetonitrile, Foreman and Whitten calculated⁴ the apparent redox potential for the $\text{Ag}^+/\text{Ag}^0(\text{aq})$ to be -1.0 V . This calculation rests on the assumption that quenching arises from full electron transfer (eq 1) and follows a Marcus correlation.

Our own experimental results suggest that Ag^0 production by electron-transfer quenching is minimal and that virtually all quenching can be attributed to exciplex formation. A brief look at the energetics involved in electron-transfer quenching is instructional. For this system



where E_{s} is the energy of solvation and is unknown. This expression, coupled with the excited state potential for the sensitizer, provides a measure of the energy barrier for electron-transfer quenching. For the aqueous case, using the diffusion-limited rate constant at 1.5 M ion strength, we find that the energy barrier must be less than 6 kcal/mol if the electron-transfer quenching rate at room temperature is to be competitive with other processes, even at 1 M Ag^+ . For acetonitrile a barrier $<7 \text{ kcal/mol}$ is required. This demand requires that the solvation of atomic silver by water be at least 17 kcal/mol and for acetonitrile the requirement is 26 kcal/mol. The observed redox potentials for Ag^+ in water and CH_3CN ¹⁹ suggest that acetonitrile is a better solvent for Ag^+ but gives little insight regarding the solvation of the atoms. However, recent ESR studies²⁰ suggest that, at low temperature, CH_3CN is not well coordinated with Ag atoms formed in situ. This infers that solvation of Ag atoms by water may not reduce the energy barrier as required and that electron transfer is not competitive energetically. Thus, the above energetic considerations support our observation that electron-transfer quenching by Ag^+ is, at best, a minor pathway.

$*\text{Ru}(\text{Me}_2\text{phen})_3^{2+}$ has a significantly more powerful reducing excited state than $*\text{Ru}(\text{bpy})_3^{2+}$ (1.01 V vs 0.84 V). Yet we see virtually identical behavior in water. We assume that the excited state is still not reducing enough to give complete electron transfer and Ag^0 . Electron-transfer quenching by Ag^+ to give Ag^0 has been observed, however. A very easily reduced Ag^+ -crown complex has been reduced by $*\text{Ru}(\text{bpy})_3^{2+}$ and other sensitizers.²¹ We attribute this reaction to the large driving force and possibly the blocking of any exciplex formation by the sterically shielding crown.

Kinnaird and Whitten²² have observed ground and excited state complexes between $\text{Ru}(\text{bpy})_2(\text{CN})_2$ and Ag^+ in acetonitrile. Stable covalent bonds are formed with bridging cyanides. Since

(16) (a) Robinson, G. W.; Frosch, R. P. *J. Chem. Phys.* **1962**, *37*, 1962. (b) Robinson, G. W.; Frosch, R. P. *J. Chem. Phys.* **1963**, *38*, 1187. Hammond, G. S. *Adv. Photochem.* **1969**, *7*, 373.

(17) (a) Caspar, J. V.; Kober, E. M.; Sullivan, B. P.; Meyer, T. J. *J. Am. Chem. Soc.* **1982**, *104*, 630. (b) Caspar, J. V.; Sullivan, B. P.; Kober, E. M.; Meyer, T. J. *J. Chem. Phys. Lett.* **1982**, *91*, 91.

(18) Demas, J. N.; Crosby, G. A. *J. Am. Chem. Soc.* **1971**, *93*, 2841.

(19) Kolthoff, I. M.; Coetzee, J. F. *J. Am. Chem. Soc.* **1957**, *79*, 1852.

(20) Symons, M. C. R.; Russell, D.; Stephens, A.; Eastland, G. *J. Chem. Soc., Faraday Trans. 1* **1986**, *82*, 2729.

(21) Humphry-Baker, R.; Graetzel, M.; Tundo, P.; Pelezzetti, E. *Angew. Chem., Int. Ed. Engl.* **1979**, *18*, 630.

(22) Kinnaird, M. G.; Whitten, D. G. *J. Chem. Phys. Lett.* **1982**, *88*, 275.

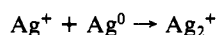
there are stable ground-state forms, these species are not exciplexes.

Thermodynamic Parameters. Only the two-equilibrium constant model successfully explains all of our data. Using the equilibrium constants determined at 25 and 6 °C, we evaluated ΔH and ΔS . These are summarized in Table II.

In keeping with many other exciplexes, we assume that the complex is stabilized largely by a charge transfer interaction. Formation of the charge transfer stabilized 1:1 $^*RuL_3^{2+}|Ag^+$ exciplex results from the affinity of Ag^+ for the electron in the partially filled π -antibonding orbitals of polypyridyl ligands.

At first, even the existence of $^*DAg_2^{2+}$ species was puzzling. The *D excited state has only a single electron promoted from a metal to a ligand π^* orbital and the electron is largely localized in a single ligand. Thus, it was difficult to envision binding of a second silver ion either to a second ligand or to the one already associated with a silver ion. Further, the ΔH for the second binding is remarkably high for an apparently unfavorable process.

We believe that this apparent anomaly can be explained by the well-known tight binding of Ag^+ to Ag^0 :



Indeed, the dimeric species is far and away the most stable form of Ag^0 in the presence of an excess of Ag^+ .⁸ Thus, we suggest that charge transfer to the first bound Ag^+ is sufficient to give considerable Ag^0 character. Then the driving force for formation of $^*DAg_2^{2+}$ is not binding of a second Ag^+ to a second ligand ring, but rather the coupling of the two silvers to form an $^*D^+|Ag_2^+$ species. Thus, the large ΔH 's arise predominantly from the silver dimerization and not from interaction with an aromatic ring.

Comparison with Other Exciplex Systems. Exciplexes have been well-studied in organic systems.²³ There is one charge transfer stabilized organic exciplex of silver ion (acceptor) with a pyrene (donor)^{24a} as well as perylene- Ag^+ exciplexes.^{24b,c} A rare termolecular excited state interaction has been proposed for the naphthalene-naphthalene-dicyanobenzene exciplex.²⁵

Much less is known about inorganic exciplexes. The only other exciplex involving a platinum metal photosensitizer appears to be $Re(phen)(CO)_3Cl$ with dimethylaniline.²⁶ Our results seem to involve the first documented case of exciplex formation involving the widely used $Ru(II)$ polypyridine photosensitizers. Further, a termolecular exciplex in inorganic systems is completely new.

Exciplexes differ widely in the relative contributions of ΔH and ΔS to their stability. In the perylene- Ag^+ -acetonitrile system, the relatively small ΔH contribution of -1 kcal/mol suggests that there is only a weak charge transfer interaction. While the -5 kcal/mol for $Ru(II)/Ag^+$ and -5.7 kcal/mol for $Re(I)/DMA$ indicates much more charge transfer. The stability of the $^*perylene/Ag^+$ exciplex is driven mainly by ΔS factors associated with the decrease in ordering of solvent around the Ag^+ upon exciplex formation. The stabilities of the $Ru(II)/Ag^+$ and $Re(I)/DMA$ exciplexes are largely due to ΔH factors, and ΔS is counterproductive. Due to the current paucity of inorganic exciplexes, it remains to be seen whether these trends will hold.

Conclusions

We report the first example of an exciplex based entirely on inorganic species. The earlier reported luminescence "quenching" by Ag^+ is shown to be incorrect and formation of both dimeric and trimeric $Ru(II)-Ag^+$ exciplexes in water accounts for all observations. Ag^0 formation was undetectable in our experiments and the yield for its formation appears to be very low (<0.02 in water and <0.05 in acetonitrile); this severely limits any practical applications of Ag^0 formed by this system.

We suspect that inorganic exciplexes will prove to be much more pervasive than the literature to date has indicated. Further, we suggest that exciplexes may make useful new, excited state reactants. Further work is in progress.

Acknowledgment. We gratefully acknowledge support by the National Science Foundation (CHE 86-00012). We thank Professor D. G. Whitten for his comments.

Registry No. $Ru(bpy)_3^{2+}$, 15158-62-0; $Ru(4,7-Me_2phen)_3^{2+}$, 24414-00-4; Ag^+ , 14701-21-4.

(23) Beens, H.; Weller, A. *Chem. Phys. Lett.* 1968, 2, 140.

(24) (a) Laeufer, A.; Dreeskamp, H.; Zachariasse, K. *Chem. Phys. Lett.* 1985, 121, 523. (b) Dreeskamp, H.; Laeufer, A.; Zander, M. *Chem. Phys. Lett.* 1984, 112, 479. (c) Laeufer, A.; Dreeskamp, H. *Ber. Bunsenges. Phys. Chem. Lett.* 1986, 90, 1195.

(25) Chandra, A. K. *Mol. Phys.* 1981, 44, 939.

(26) Vogler, A.; Kunkley, H. *Inorg. Chim. Acta* 1980, 45, L265.

Chiral Synthesis via Organoboranes. 12. Conversion of Boronic Esters of Essentially 100% Optical Purity into Monoalkylhexylboranes Providing Convenient Synthetic Routes to *trans*-Olefins, *cis*-Olefins, Alkynes, and Ketones of Very High Enantiomeric Purities

Herbert C. Brown,* Raman K. Bakshi,¹ and Bakthan Singaram¹

Contribution from the H. C. Brown and R. B. Wetherill Laboratories of Chemistry, Purdue University, West Lafayette, Indiana 47907. Received June 8, 1987

Abstract: 2-Alkyl-1,3,2-dioxaborinanes $R^*BO_2(CH_2)_3$ of essentially 100% optical purity, prepared by the asymmetric hydroboration of readily available prochiral olefins with subsequent removal of the chiral auxiliary, can be transformed into the lithium monoalkylborohydrides R^*BH_3Li of essentially 100% ee by reaction with lithium aluminum hydride. These monoalkylborohydrides are converted into optically active monoalkylhexylboranes R^*ThxBH through the intermediate formation of the corresponding optically active monoalkylboranes R^*BH_2 . The synthetic potential of optically active R^*ThxBH is demonstrated by carrying out various reactions leading to *trans*-olefins, *cis*-olefins, alkynes, and ketones of very high optical purities. Since both (+)- and (-)-alkylboronic esters are available in essentially 100% optical purity, it is now possible to synthesize (+)- and (-)-*cis*- and *trans*-olefins, -alkynes, and -ketones in very high optical purities.

Organoboranes have become one of the most significant classes of organometallics in organic synthesis.² Our studies have es-

tablished that organoboranes transfer the alkyl group to essentially most other elements of synthetic interest, including carbon, with